

## 19 Baroclinic Instability

### 19.1 Quasi-geostrophic theory

We now discuss baroclinic instability within the context of quasi-geostrophic theory. The form of quasi-geostrophic theory which uses the pseudo-height  $z = (c_p \theta_0 / g) [1 - (p/p_0)^{R/c_p}]$  as vertical coordinate was discussed in Chapter 13. Recall that the most concise form of quasi-geostrophic theory consists of the prognostic equation for potential vorticity, the invertibility principle, and the boundary conditions, i.e.,

$$\frac{\partial q}{\partial t} + u_g \frac{\partial q}{\partial x} + v_g \frac{\partial q}{\partial y} = 0, \quad (19.1)$$

$$q = f + \frac{\partial^2 \psi}{\partial x^2} + \frac{\partial^2 \psi}{\partial y^2} + \frac{\partial}{\rho \partial z} \left( \frac{\rho f^2}{N^2} \frac{\partial \psi}{\partial z} \right), \quad (19.2)$$

$$\left( \frac{\partial}{\partial t} + u_g \frac{\partial}{\partial x} + v_g \frac{\partial}{\partial y} \right) \frac{\partial \psi}{\partial z} = 0, \quad \text{at } z = 0, z_T, \quad (19.3)$$

where

$$u_g = -\frac{\partial \psi}{\partial y}, \quad v_g = \frac{\partial \psi}{\partial x}, \quad (19.4)$$

are the geostrophic wind components,  $\rho(z)$  the pseudo-density (a known function of  $z$ ), and  $N^2(z)$  the square of the Brunt-Väisälä frequency (also a known function of  $z$ ),  $\psi = \phi/f$  the geostrophic streamfunction,  $z = 0$  the bottom and  $z = z_T$  the top of the model atmosphere. Equations (19.1)–(19.4) form a closed system in the four dependent variables  $q(x, y, z, t)$ ,  $u_g(x, y, z, t)$ ,  $v_g(x, y, z, t)$ ,  $\psi(x, y, z, t)$ . Equation (19.1) predicts the quasi-geostrophic potential vorticity in the interior of the fluid. Equation (19.2) is the quasi-geostrophic invertibility relation and is used to obtain  $\psi(x, y, z, t)$  from  $q(x, y, z, t)$ . Since (19.2) is a second order elliptic partial differential equation, boundary conditions at the top and bottom are required (in addition to  $q$  in the fluid interior) to solve it. These time-varying boundary conditions are determined by (19.3), which is the thermodynamic equation applied at the boundaries.

### 19.2 The Charney-Stern necessary condition for combined barotropic-baroclinic instability

Now consider linearized motions about the basic state geostrophic zonal flow  $\bar{u}(y, z)$ . The linearized versions of (19.1), (19.2) and (19.3) are

$$\frac{\partial q'}{\partial t} + \bar{u} \frac{\partial q'}{\partial x} + \frac{\partial \psi'}{\partial x} \frac{\partial \bar{q}}{\partial y} = 0, \quad (19.5)$$

$$q' = \frac{\partial^2 \psi'}{\partial x^2} + \frac{\partial^2 \psi'}{\partial y^2} + \frac{\partial}{\rho \partial z} \left( \frac{\rho f^2}{N^2} \frac{\partial \psi'}{\partial z} \right), \quad (19.6)$$

$$\left( \frac{\partial}{\partial t} + \bar{u} \frac{\partial}{\partial x} \right) \frac{\partial \psi'}{\partial z} - \frac{\partial \psi'}{\partial x} \frac{\partial \bar{u}}{\partial z} = 0 \quad \text{at } z = 0, z_T. \quad (19.7)$$

Notice that, if the basic state is barotropic (i.e.,  $\partial \bar{u} / \partial z = 0$ ), and if there are no potential temperature perturbations (i.e.,  $\partial \psi' / \partial z = 0$ ), then (19.7) is trivially satisfied and the last term in (19.6) disappears, resulting in the barotropic instability problem studied in the last chapter. When  $\bar{u}$  is a function of both  $y$  and  $z$ , we have the possibility of combined barotropic-baroclinic instability.

Substituting the assumed form of solution

$$\psi'(x, y, z, t) = \Psi(y, z) e^{ik(x-ct)} \quad (19.8)$$

into (19.5)–(19.7), we obtain

$$\left[ \frac{\partial^2 \Psi}{\partial y^2} - k^2 \Psi + \frac{\partial}{\rho \partial z} \left( \frac{\rho f^2}{N^2} \frac{\partial \Psi}{\partial z} \right) \right] + \frac{\partial \bar{q}}{\partial y} \left( \frac{\bar{u} - c^*}{|\bar{u} - c|^2} \right) \Psi = 0, \quad (19.9)$$

$$\frac{\partial \Psi}{\partial z} = \frac{\partial \bar{u}}{\partial z} \left( \frac{\bar{u} - c^*}{|\bar{u} - c|^2} \right) \Psi \quad \text{at } z = 0, z_T. \quad (19.10)$$

Taking the complex conjugate of (19.9) and (19.10), we obtain

$$\left[ \frac{\partial^2 \Psi^*}{\partial y^2} - k^2 \Psi^* + \frac{\partial}{\partial z} \left( \frac{\rho f^2}{N^2} \frac{\partial \Psi^*}{\partial z} \right) \right] + \frac{\partial \bar{q}}{\partial y} \left( \frac{\bar{u} - c}{|\bar{u} - c|^2} \right) \Psi^* = 0, \quad (19.11)$$

$$\frac{\partial \Psi^*}{\partial z} = \frac{\partial \bar{u}}{\partial z} \left( \frac{\bar{u} - c}{|\bar{u} - c|^2} \right) \Psi^* \quad \text{at} \quad z = 0, z_T. \quad (19.12)$$

Multiplying (19.9) by  $\Psi^*$  and (19.11) by  $\Psi$ , and then taking the difference of these two results, we obtain

$$\frac{\partial}{\partial y} \left( \Psi^* \frac{\partial \Psi}{\partial y} - \Psi \frac{\partial \Psi^*}{\partial y} \right) + \frac{\partial}{\partial z} \left( \Psi^* \frac{\rho f^2}{N^2} \frac{\partial \Psi}{\partial z} - \Psi \frac{\rho f^2}{N^2} \frac{\partial \Psi^*}{\partial z} \right) + \frac{\partial \bar{q}}{\partial y} \frac{2ic_i}{|\bar{u} - c|^2} |\Psi|^2 = 0, \quad (19.13)$$

We now multiply (19.13) by  $\rho$  and integrate over  $y$  and  $z$ . The flow is assumed to be confined within a zonal channel, with  $\Psi = 0$  and  $\Psi^* = 0$  on the northern and southern edges of the channel. The integration then yields

$$\int \left[ \frac{\rho f^2}{N^2} \left( \Psi^* \frac{\partial \Psi}{\partial z} - \Psi \frac{\partial \Psi^*}{\partial z} \right) \right]_0^{z_T} dy + 2ic_i \iint \frac{\partial \bar{q}}{\partial y} \frac{|\Psi|^2}{|\bar{u} - c|^2} \rho dy dz = 0. \quad (19.14)$$

The first term in (19.14) can be rewritten using the boundary conditions (19.10) and (19.12). Multiplying (19.10) by  $\Psi^*$  and (19.12) by  $\Psi$ , and then taking the difference of these two results, we obtain

$$\Psi^* \frac{\partial \Psi}{\partial z} - \Psi \frac{\partial \Psi^*}{\partial z} = \frac{\partial \bar{u}}{\partial z} \frac{2ic_i}{|\bar{u} - c|^2} |\Psi|^2. \quad (19.15)$$

Using (19.15) in (19.14), we obtain

$$c_i \left\{ \int \left[ \frac{\rho f^2}{N^2} \frac{\partial \bar{u}}{\partial z} \frac{|\Psi|^2}{|\bar{u} - c|^2} \right]_0^{z_T} dy + \iint \frac{\partial \bar{q}}{\partial y} \frac{|\Psi|^2}{|\bar{u} - c|^2} \rho dy dz \right\} = 0. \quad (19.16)$$

For unstable waves ( $c_i \neq 0$ ), the term in braces must vanish, which is the Charney-Stern necessary condition for combined barotropic-baroclinic instability. This means that a necessary condition for instability is that the functions  $\partial \bar{q} / \partial y$ ,  $(\partial \bar{\theta} / \partial y)_{z=0}$ ,  $-(\partial \bar{\theta} / \partial y)_{z=z_T}$  cannot all have the same sign everywhere in  $(y, z)$ . We can distinguish two different types of instability: Eady-type (or boundary-type) instability and internal-type instability.

Eady-type instability can occur when  $\partial \bar{q} / \partial y = 0$  in the interior of the fluid. The Charney-Stern necessary condition for instability then reduces to

$$\int \left[ \frac{\rho f^2}{N^2} \frac{\partial \bar{u}}{\partial z} \frac{|\Psi|^2}{|\bar{u} - c|^2} \right]_0^{z_T} dy = 0. \quad (19.17)$$

Since  $|\Psi|^2 \geq 0$ ,  $|\bar{u} - c|^2 \geq 0$ , and  $\rho > 0$ , (19.17) requires that  $(\partial \bar{\theta} / \partial y)_{z=0}$  have the same sign as  $(\partial \bar{\theta} / \partial y)_{z=z_T}$ .

Internal barotropic-baroclinic instability can possibly occur when  $(\partial \bar{\theta} / \partial y)_{z=0}$  and  $(\partial \bar{\theta} / \partial y)_{z=z_T}$  both vanish. The Charney-Stern necessary condition for instability then reduces to

$$\iint \frac{\partial \bar{q}}{\partial y} \frac{|\Psi|^2}{|\bar{u} - c|^2} \rho dy dz = 0. \quad (19.18)$$

Since  $|\Psi|^2 \geq 0$ ,  $|\bar{u} - c|^2 \geq 0$ , and  $\rho > 0$ , (19.18) requires that  $\partial \bar{q} / \partial y$  have both signs in the interior of the fluid.

Burpee (1972) investigated the origin and structure of easterly waves that form in the lower troposphere of North Africa. He argued that these waves are directly related to the mid-tropospheric easterly jet (now usually referred to as the African easterly jet) that is found within the baroclinic zone to the south of the Sahara. This zonal flow is rather unique because easterlies increase with height and warm air lies to the north. A north-south cross section of the African easterly jet is shown in Fig. 19.1, which depicts the August mean zonal flow. The jet is centered at approximately 600 mb and 15 N. Burpee also constructed the August mean meridional cross section of potential vorticity  $\bar{q}(y, z)$ , which is shown in Fig. 19.2. Note that, as you proceed poleward from the equator at 600 mb, the potential vorticity increases to approximately 12 N and then decreases. Thus,  $\partial \bar{q} / \partial y$  has both signs, and the necessary condition (19.18) is satisfied.

In 1974 a large international field program called GATE (Global Atmospheric Research Program Atlantic Tropical Experiment) was conducted in the region of the eastern Atlantic and west Africa. Reed et al. (1977) carefully examined this dataset for the period 23 August–19 September 1974, during which 8 easterly waves propagated across the region.

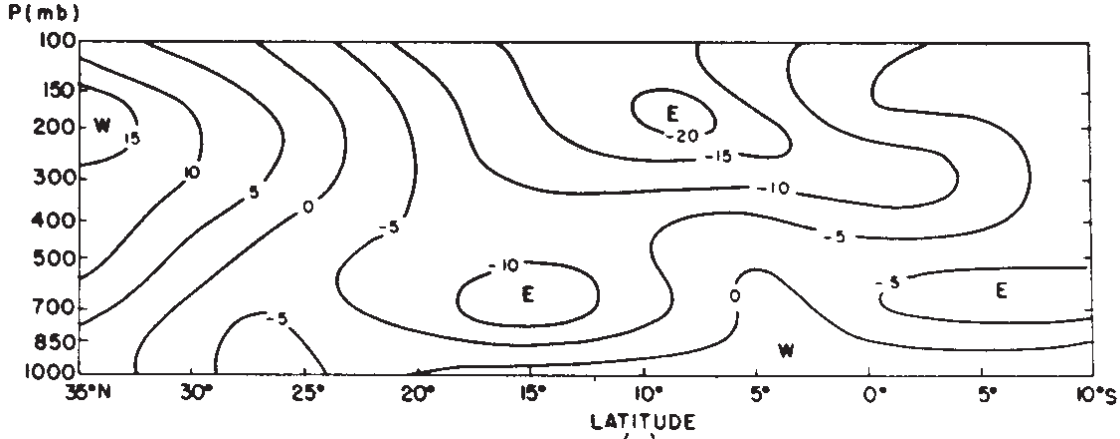


Figure 19.1: August mean meridional cross section of zonal wind. The African easterly jet is centered at approximately 600 mb and 15 N. From Burpee (1972).

A 700 mb streamline map of one of these easterly waves is shown in Fig. 19.3. The mean wavelength of the 8 waves was 2500 km and the mean period was 3.5 days (i.e., the waves propagate westward at  $8 \text{ ms}^{-1}$ , or 6–7 degrees longitude per day). Reed et al. made mean meridional cross sections with respect to the E-W axis of each wave (e.g., the E-W line at approximately 11 N in Fig. 19.3. The mean cross sections for zonal wind, absolute vorticity, temperature and relative humidity are shown in Fig. 19.4. The shaded region in Fig. 19.4b shows where the meridional gradient of absolute vorticity is reversed. Thus, the necessary condition for barotropic instability is satisfied. Note that the troughs and ridges in Fig. 19.3 have a northeast to southwest tilt. This tilt is against the horizontal shear of the basic flow, which has strong easterlies at 17 N, as depicted in Fig. 19.4a. Such a wave tilt against the basic state horizontal shear is characteristic of barotropic instability, as shown in Fig. 18.1 of Chapter 18. However, it should be noted that our adiabatic stability arguments are only part of the whole story because easterly waves are often embedded with strong cumulus convection.

In the next section we shall isolate the baroclinic instability process by considering  $\bar{u}$  to be a function of  $z$  only. The simplest in this class of pure baroclinic instability problems is the Eady problem, in which  $\bar{u}(z)$  is a linear function of  $z$  (i.e.,  $\partial\bar{u}/\partial z$  is a constant).

### 19.3 The Eady problem

In what follows we shall assume  $f$  is a constant (the  $f$ -plane approximation),  $N^2$  is a constant, and  $\rho$  is a constant (the Boussinesq approximation). For the Eady problem,  $\bar{u}_g$  does not depend on  $y$  and is a linear function of  $z$ , i.e.,  $\bar{u}_g = \Lambda z$ , where  $\Lambda$  is the constant vertical shear. The basic state potential vorticity is uniform and we obtain  $q' = 0$  from (19.5), i.e., the Eady wave has no potential vorticity anomaly in the interior of the fluid. In summary, the Eady problem is

$$\frac{\partial^2 \phi'}{\partial x^2} + \frac{\partial^2 \phi'}{\partial y^2} + \frac{f^2}{N^2} \frac{\partial^2 \phi'}{\partial z^2} = 0, \tag{19.19}$$

$$\left( \frac{\partial}{\partial t} + \Lambda z \frac{\partial}{\partial x} \right) \frac{\partial \phi'}{\partial z} - \Lambda \frac{\partial \phi'}{\partial x} = 0 \quad \text{at} \quad z = -H, H. \tag{19.20}$$

To solve (19.19) and (19.20) we first note that the solution of (19.19) is

$$\phi'(x, y, z, t) = [A \sinh(\kappa z) + B \cosh(\kappa z)] \cos(l y) e^{ik(x-ct)}, \tag{19.21}$$

where  $A$  and  $B$  are complex constants and  $\kappa = (N/f)(k^2 + l^2)^{1/2}$ . Substituting (19.21) into (19.20) yields

$$(\Lambda H - c)\kappa [A \cosh(\kappa H) + B \sinh(\kappa H)] - \Lambda [A \sinh(\kappa H) + B \cosh(\kappa H)] = 0, \tag{19.22}$$

$$(\Lambda H + c)\kappa [A \cosh(\kappa H) - B \sinh(\kappa H)] - \Lambda [A \sinh(\kappa H) - B \cosh(\kappa H)] = 0. \tag{19.23}$$

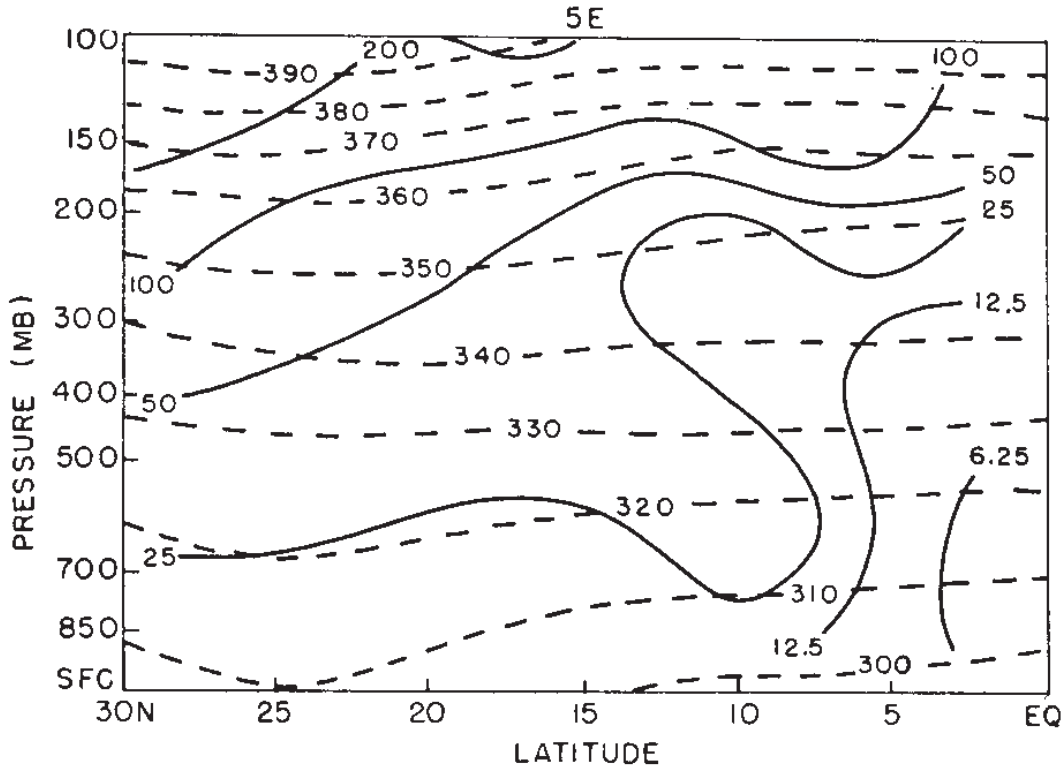


Figure 19.2: August mean meridional cross section of potential temperature (dashed lines labeled in degrees Kelvin) and potential vorticity  $\bar{q}(y, z)$ . From Burpee (1972).

Taking the sum and difference of (19.22) and (19.23) we obtain the simpler system

$$\left( \coth(\kappa H) - \frac{1}{\kappa H} \right) A - \left( \frac{c}{\Lambda H} \right) B = 0, \tag{19.24}$$

$$- \left( \frac{c}{\Lambda H} \right) A + \left( \tanh(\kappa H) - \frac{1}{\kappa H} \right) B = 0. \tag{19.25}$$

For a nontrivial solution of this algebraic system in  $A$  and  $B$  we must have

$$c^2 = (\Lambda H)^2 \left( \tanh(\kappa H) - \frac{1}{\kappa H} \right) \left( \coth(\kappa H) - \frac{1}{\kappa H} \right). \tag{19.26}$$

When the eigenvalue relation (19.26) is substituted back into (19.24) or (19.25), we obtain

$$\frac{A}{B} = \left( \frac{\tanh(\kappa H) - (\kappa H)^{-1}}{\coth(\kappa H) - (\kappa H)^{-1}} \right)^{1/2}. \tag{19.27}$$

When this result is used in (19.21) we obtain

$$\phi'(x, y, z, t) = B \left[ \cosh(\kappa z) + \left( \frac{\tanh(\kappa H) - (\kappa H)^{-1}}{\coth(\kappa H) - (\kappa H)^{-1}} \right)^{1/2} \sinh(\kappa z) \right] \cos(ly) e^{ik(x-ct)}. \tag{19.28}$$

Equations (19.26) and (19.28) are our main results so far, with (19.26) giving the two eigenvalues and (19.28) giving an eigenfunction corresponding to each eigenvalue. Note that the constant  $B$  remains undetermined because in general eigenfunctions are only determined to within a multiplicative constant.

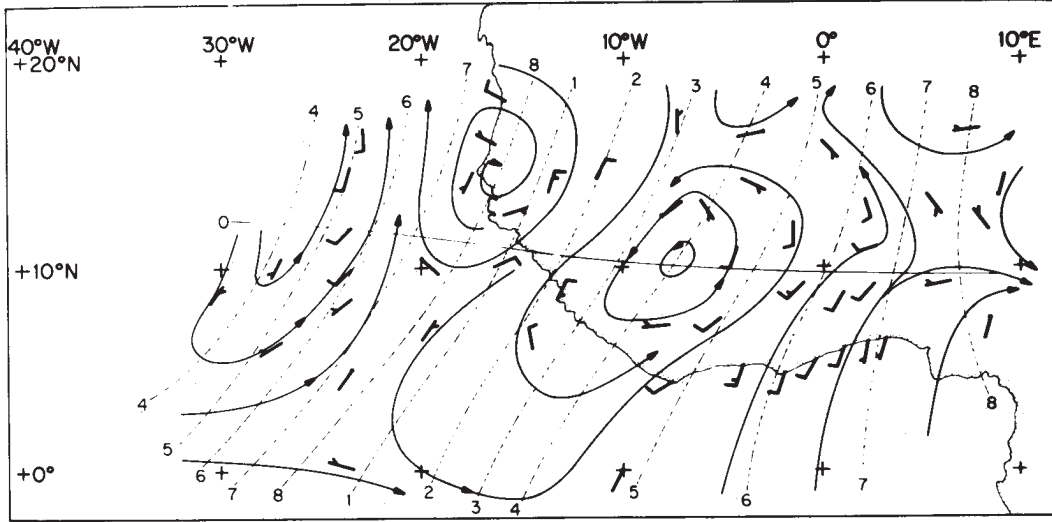


Figure 19.3: Streamline analysis for 1200 UTC 7 September 1974. One full barb corresponds to  $5 \text{ ms}^{-1}$ , one-half barb to  $2.5 \text{ ms}^{-1}$ , and no barb to  $1 \text{ ms}^{-1}$ . From Reed et al. (1977).

The two eigenvalues determined from (19.26) are either both real or both pure imaginary. In the latter case the eigenvalues are  $c = ic_i$  and the factor  $e^{ik(x-ct)}$  in (19.28) can be written as  $e^{ikx}e^{kc_it}$ , so that  $kc_i$  is the growth rate, with  $c_i > 0$  corresponding to growing waves and  $c_i < 0$  corresponding to damping waves. Since  $\coth(\kappa H) - (\kappa H)^{-1} > 0$ , we conclude from (19.26) that instability occurs when  $\tanh(\kappa H) - (\kappa H)^{-1} < 0$ , which corresponds to  $\kappa H < 1.1997$ . In other words

$$\frac{NH}{f}(k^2 + l^2)^{1/2} < 1.1997 \quad \text{for instability.}$$

The unstable region of the  $(k, l)$ -plane is enclosed by the circle in Fig. 19.5, and since

$$c_i = \pm \Lambda H \left[ \left( \frac{1}{\kappa H} - \tanh(\kappa H) \right) \left( \coth(\kappa H) - \frac{1}{\kappa H} \right) \right]^{1/2} \quad (19.29)$$

in this region, there occurs both a growing and a damping mode (i.e., the eigenvalues  $c$  occur in conjugate pairs). We generally concentrate our attention on the growing modes and ignore the damping modes since the growing modes must eventually dominate the total solution. In fact, we generally concentrate on only the fastest growing mode since it will be “naturally selected” from the other growing modes. Isolines of the growth rate  $kc_i$ , for the positive  $c_i$  root computed using (19.29), are shown in Fig. 19.5. Note that the maximum growth rate occurs for  $l = 0$  (i.e., on the  $k$  axis in Fig. 19.5). To pinpoint the value of  $k$  yielding maximum instability, let us consider (19.29) with  $l = 0$ . Then, defining  $\eta = NHk/f$ , we have

$$kc_i = \frac{f\Lambda}{N} [(1 - \eta \tanh \eta)(\eta \coth \eta - 1)]^{1/2}. \quad (19.30)$$

From (19.30) we find that  $d(kc_i)/d\eta = 0$  when

$$(1 - \eta \tanh \eta) \left( \coth \eta - \frac{\eta}{\sinh^2 \eta} \right) = (\eta \coth \eta - 1) \left( \tanh \eta + \frac{\eta}{\cosh^2 \eta} \right). \quad (19.31)$$

Multiplying this out and noting that the terms in  $\eta^2$  cancel, we obtain

$$\eta = \frac{\tanh \eta + \coth \eta}{\tanh^2 \eta + \coth^2 \eta}. \quad (19.32)$$

This transcendental equation in  $\eta$  has the solution  $\eta \approx 0.8031$ , or equivalently  $NHk/f = 0.8031$ . Substitution of this value of  $\eta$  into (19.30) yields  $(kc_i)_{\max} \approx 0.3098(f/N)\Lambda$ . For  $(N/f) = 100$ ,  $H = 5 \text{ km}$ , and  $\Lambda = 3 \times 10^{-3} \text{ s}^{-1}$

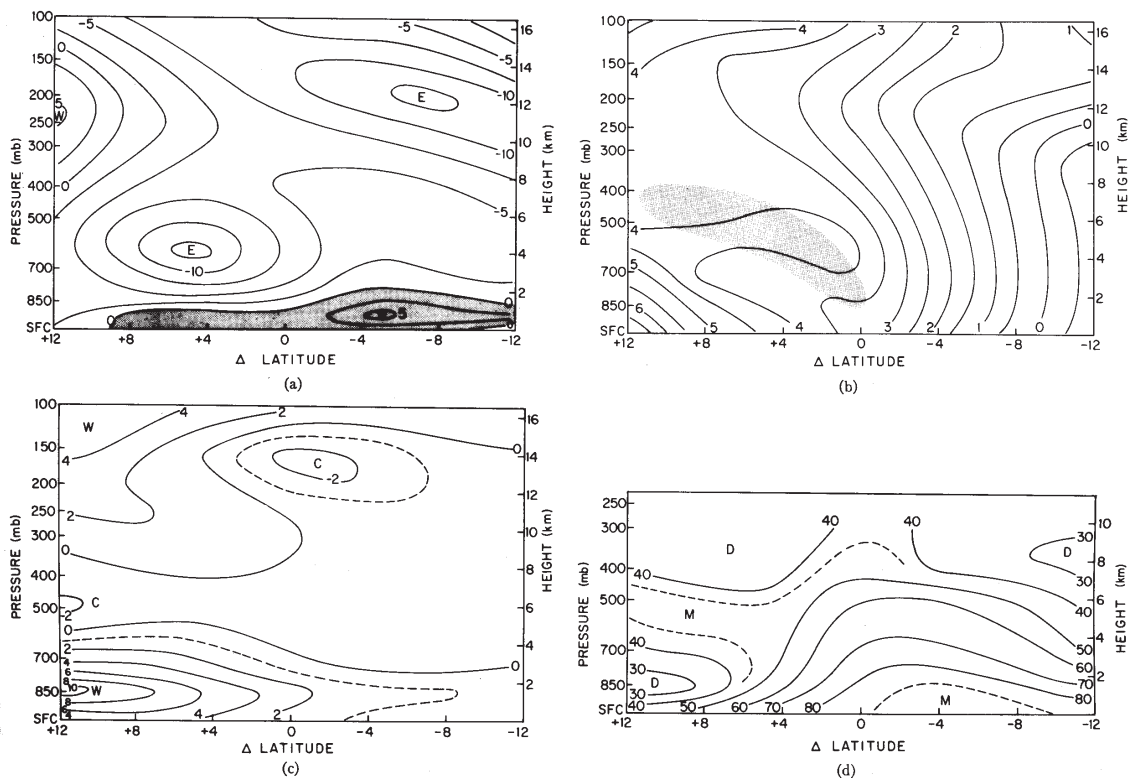


Figure 19.4: Zonal mean fields for GATE. “Zero” latitude is approximately 11 N over land and 12 N over ocean. (a) Zonal wind ( $\text{ms}^{-1}$ ); (b) absolute vorticity ( $10^{-5}\text{s}^{-1}$ ); (c) temperature deviations (degrees Celsius) from the sounding at  $\Delta$  latitude =  $-12$ ; (d) relative humidity (percent). From Reed et al. (1977).

(i.e., a vertical shear of  $30 \text{ ms}^{-1}$  over a depth of 10 km), the wavelength of maximum instability is 3912 km and the  $e$ -folding time is 29.9 hours.

For the fastest growing mode, (19.27) simplifies to

$$\frac{A}{B} = i \left( \frac{1 - \eta \tanh \eta}{\eta \coth \eta - 1} \right)^{1/2} = i \coth \eta, \quad (19.33)$$

where the last equality in (19.33) follows from the use of (19.32). Then, defining  $C = iB \cosh(NHk/f)$ , the real part of the eigenfunction (19.21), or equivalently (19.28), reduces to

$$\phi'(x, y, z, t) = C \left[ \cos(kx) \frac{\sinh(Nkz/f)}{\sinh(NkH/f)} + \sin(kx) \frac{\cosh(Nkz/f)}{\cosh(NkH/f)} \right] e^{kc_i t}, \quad (19.34)$$

from which we can easily calculate the potential temperature perturbation (proportional to  $\partial\phi'/\partial z$ ) and the meridional wind perturbation (proportional to  $\partial\phi'/\partial x$ ). The structure of the most unstable mode, as determined by (19.34), is shown in Fig. 19.6.

To illustrate the horizontal structure of the Eady wave, geopotential anomaly contours and temperature contours for a growing square ( $k = l$ ) Eady wave at the steering level are shown in Fig. 19.7.

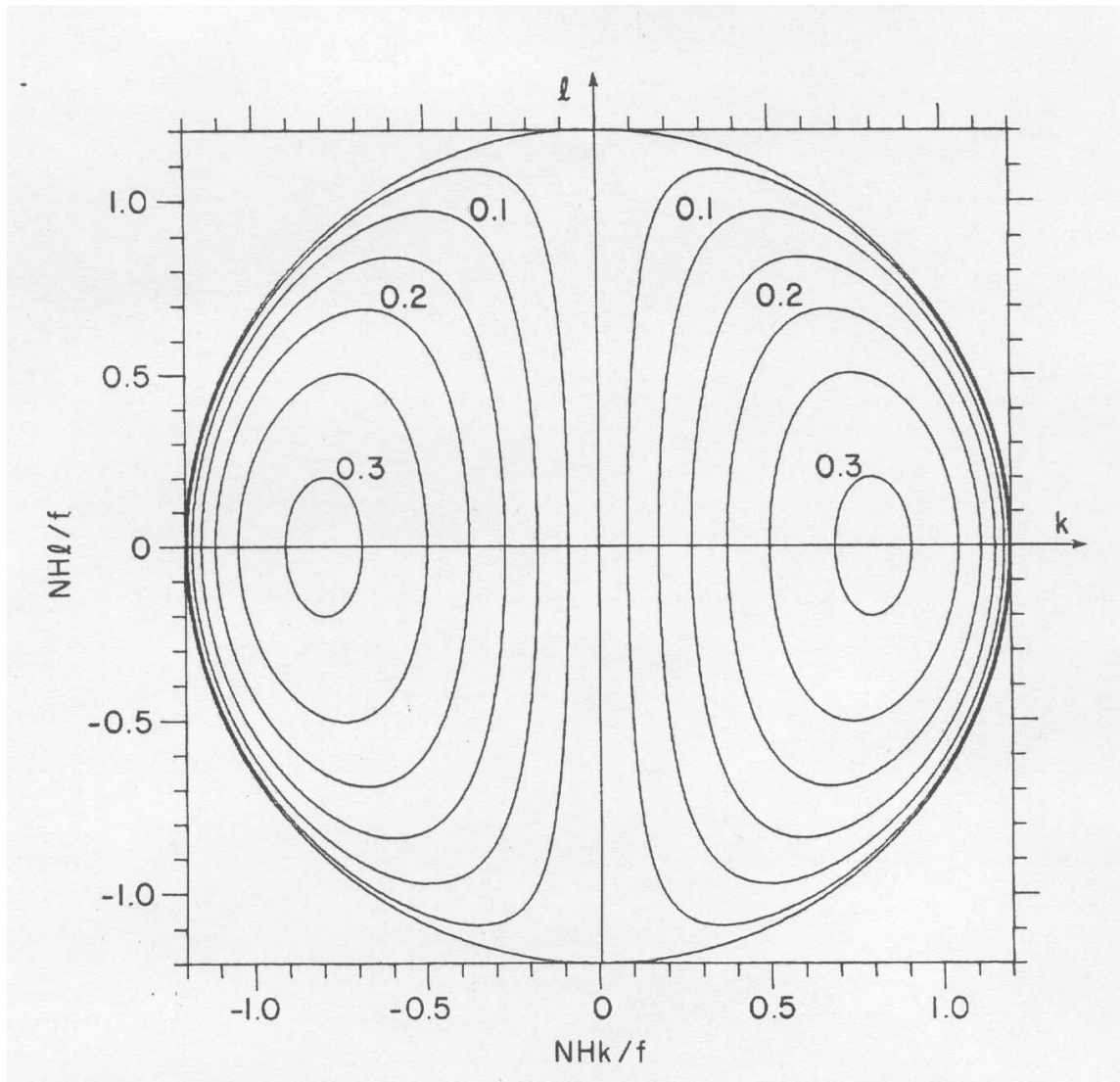


Figure 19.5: Isolines of the growth rate  $kc_i$  for an Eady wave as a function of the horizontal wavenumbers  $k$  and  $l$ . The zero isoline occurs when  $k = 0$  and when  $(N/f)H(k^2 + l^2)^{1/2} \approx 1.1997$ . The maximum growth rate occurs at wavenumbers  $NHk/f \approx 0.8031$  and  $l = 0$ , where the growth rate is  $(kc_i)_{\max} \approx 0.3098(f/N)\Lambda$ . From Gill 1982.

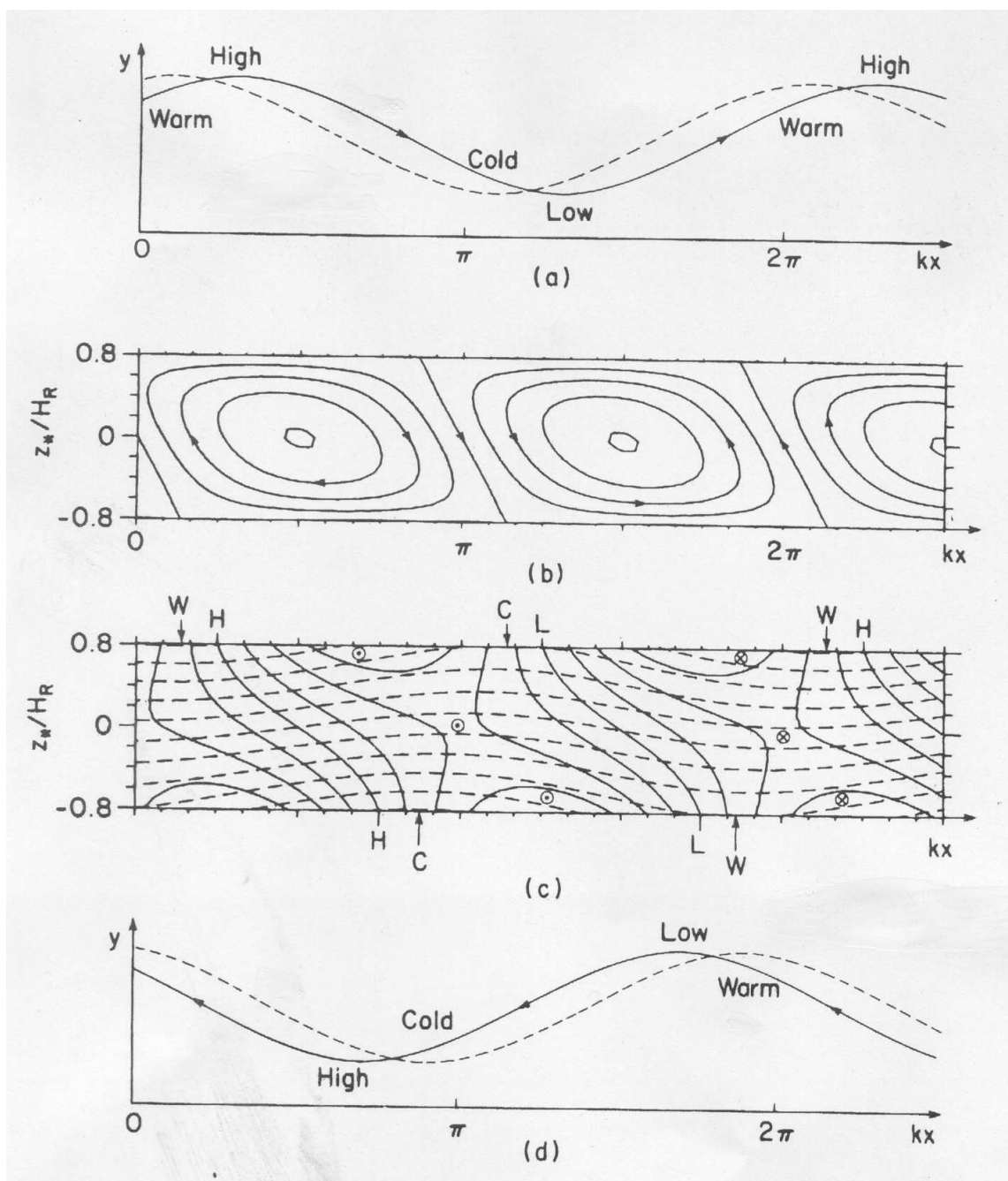


Figure 19.6: Structure of the most unstable Eady wave, as determined by (19.34). The most unstable wave is independent of  $y$  and its horizontal structure at the upper boundary is shown in (a) and at the lower boundary in (d). The phase shift between the pressure field and the temperature field at the boundaries is  $21^\circ$ . The streamfunction for the ageostrophic flow in the  $x, z$  plane is shown in (b). In (c), the dashed lines indicate the potential temperature surfaces and the solid lines the meridional component of the wind, with flow into the page denoted by  $\otimes$  and flow out of the page by  $\odot$ . Note that colder air is moving southward and warmer air northward, so there is a net poleward heat flux. The phase lines for the  $v$  field tilt westward with height, with a  $90^\circ$  westward phase shift between the bottom and top. From Gill 1982.

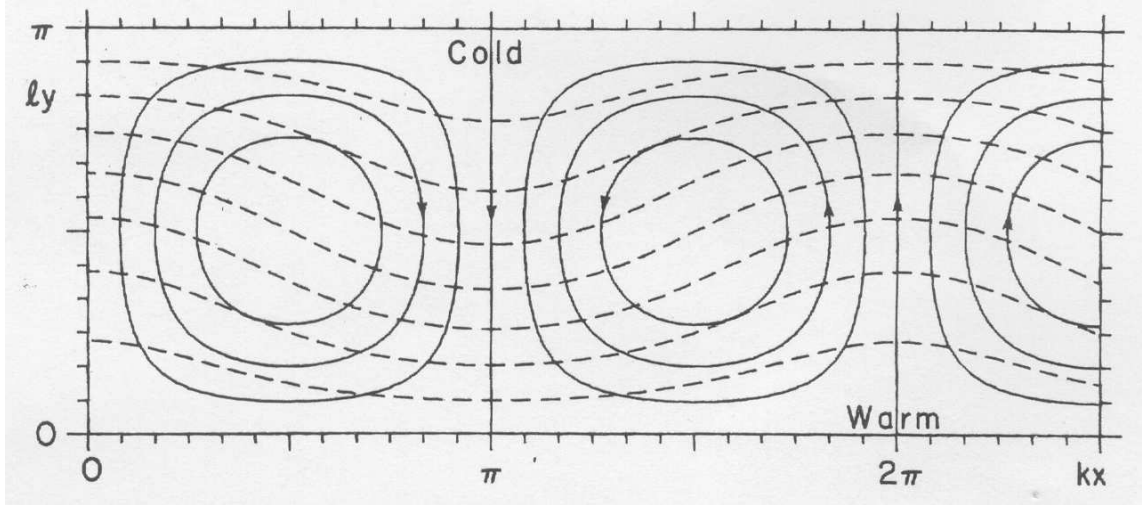


Figure 19.7: Geopotential anomaly contours (solid) and temperature contours (dashed) for a growing square ( $k = l$ ) Eady wave at the steering level. From Gill 1982.

### 19.4 The two-layer model

Consider quasi-geostrophic flow on an  $f$ -plane. The two-layer model for such a flow is

$$\frac{\partial q_1}{\partial t} - \frac{\partial \psi_1}{\partial y} \frac{\partial q_1}{\partial x} + \frac{\partial \psi_1}{\partial x} \frac{\partial q_1}{\partial y} = 0, \quad (19.35)$$

$$\frac{\partial q_2}{\partial t} - \frac{\partial \psi_2}{\partial y} \frac{\partial q_2}{\partial x} + \frac{\partial \psi_2}{\partial x} \frac{\partial q_2}{\partial y} = 0, \quad (19.36)$$

$$q_1 = f + \nabla^2 \psi_1 - \mu^2 (\psi_1 - \psi_2), \quad (19.37)$$

$$q_2 = f + \nabla^2 \psi_2 + \mu^2 (\psi_1 - \psi_2), \quad (19.38)$$

where  $q_1$  and  $\psi_1$  are the quasi-geostrophic potential vorticity and streamfunction in the upper layer, and  $q_2$  and  $\psi_2$  are the corresponding fields in the lower layer. The constant  $\mu$  is the inverse of the Rossby length. Equations (19.35)–(19.38) constitute a system of four equations in the four unknowns  $q_1(x, y, t)$ ,  $q_2(x, y, t)$ ,  $\psi_1(x, y, t)$  and  $\psi_2(x, y, t)$ .

We now linearize (19.35)–(19.38) about a zonal flow which is a constant westerly  $U$  in the upper layer and a constant easterly  $-U$  in the lower layer. Thus,  $q_1(x, y, t) = \bar{q}_1(y) + q'_1(x, y, t)$  and  $\psi_1(x, y, t) = \bar{\psi}_1(y) + \psi'_1(x, y, t)$ , with similar relations for  $q_2(x, y, t)$  and  $\psi_2(x, y, t)$ , where  $\bar{u}_1 = -d\bar{\psi}_1/dy = U$  and  $\bar{u}_2 = -d\bar{\psi}_2/dy = -U$ . It is easily shown from (19.37) and (19.38) that  $\bar{q}_1 = f - \mu^2(\bar{\psi}_1 - \bar{\psi}_2)$  and  $\bar{q}_2 = f + \mu^2(\bar{\psi}_1 - \bar{\psi}_2)$ , so that the poleward gradients of basic state potential vorticity in the upper and lower layers are given by  $d\bar{q}_1/dy = 2U\mu^2$  and  $d\bar{q}_2/dy = -2U\mu^2$ . The reversal of the poleward gradient of basic state potential vorticity in the lower layer allows counterpropagating Rossby waves in the two layers, which (as we shall see below) leads to baroclinic instability. The linearized versions of (19.35)–(19.38) are

$$\frac{\partial q'_1}{\partial t} + U \frac{\partial q'_1}{\partial x} + \bar{q}_{1y} \frac{\partial \psi'_1}{\partial x} = 0, \quad (19.39)$$

$$\frac{\partial q'_2}{\partial t} - U \frac{\partial q'_2}{\partial x} - \bar{q}_{1y} \frac{\partial \psi'_2}{\partial x} = 0, \quad (19.40)$$

$$q'_1 = \nabla^2 \psi'_1 - \mu^2 (\psi'_1 - \psi'_2), \quad (19.41)$$

$$q'_2 = \nabla^2 \psi'_2 + \mu^2 (\psi'_1 - \psi'_2). \quad (19.42)$$

Equations (19.39)–(19.42) constitute a linear system of four equations in the four unknowns  $q'_1(x, y, t)$ ,  $q'_2(x, y, t)$ ,  $\psi'_1(x, y, t)$  and  $\psi'_2(x, y, t)$ .

We now search for solutions of (19.39)–(19.42) having the form  $q'_1(x, y, t) = \hat{q}_1 e^{ik(x-ct)} \sin(l y)$  and  $\psi'_1(x, y, t) = \hat{\psi}_1 e^{ik(x-ct)} \sin(l y)$ , with similar forms for  $q'_2(x, y, t)$  and  $\psi'_2(x, y, t)$ . Substituting these into (19.39)–(19.42) we obtain the following four algebraic equations for the complex constants  $\hat{q}_1$ ,  $\hat{\psi}_1$ ,  $\hat{q}_2$  and  $\hat{\psi}_2$ :

$$(c - U)\hat{q}_1 - \bar{q}_{1y}\hat{\psi}_1 = 0, \tag{19.43}$$

$$(c + U)\hat{q}_2 + \bar{q}_{1y}\hat{\psi}_2 = 0, \tag{19.44}$$

$$\hat{q}_1 = -(k^2 + l^2 + \mu^2)\hat{\psi}_1 + \mu^2\hat{\psi}_2, \tag{19.45}$$

$$\hat{q}_2 = \mu^2\hat{\psi}_1 - (k^2 + l^2 + \mu^2)\hat{\psi}_2. \tag{19.46}$$

To reduce the algebraic system (19.43)–(19.46) to a system in two unknowns, we have a choice. We can eliminate  $\hat{q}_1$  and  $\hat{q}_2$  to obtain a system in  $\hat{\psi}_1$  and  $\hat{\psi}_2$ , or we can eliminate  $\hat{\psi}_1$  and  $\hat{\psi}_2$  to obtain a system in  $\hat{q}_1$  and  $\hat{q}_2$ . We choose the latter. This can be accomplished by first solving (19.45) and (19.46) for  $\hat{\psi}_1$  and  $\hat{\psi}_2$  in terms of  $\hat{q}_1$  and  $\hat{q}_2$ , and then substituting the results into (19.43) and (19.44). Thus, solving (19.45) and (19.46) for  $\hat{\psi}_1$  and  $\hat{\psi}_2$  in terms of  $\hat{q}_1$  and  $\hat{q}_2$ , we obtain

$$-(k^2 + l^2)\hat{\psi}_1 = \left( \frac{k^2 + l^2 + \mu^2}{k^2 + l^2 + 2\mu^2} \right) \hat{q}_1 + \left( \frac{\mu^2}{k^2 + l^2 + 2\mu^2} \right) \hat{q}_2, \tag{19.47}$$

$$-(k^2 + l^2)\hat{\psi}_2 = \left( \frac{\mu^2}{k^2 + l^2 + 2\mu^2} \right) \hat{q}_1 + \left( \frac{k^2 + l^2 + \mu^2}{k^2 + l^2 + 2\mu^2} \right) \hat{q}_2. \tag{19.48}$$

Equations (19.47) and (19.48) constitute the spectral space solution of the invertibility principle, with (19.47) giving the vorticity in the upper layer in terms of the potential vorticity in both layers and (19.48) giving the vorticity in the lower layer in terms of the potential vorticity in both layers. There are two interesting limits. For disturbances whose horizontal scale is much smaller than the Rossby length ( $k^2 + l^2 \gg 2\mu^2$ ), (19.47) and (19.48) reduce to  $-(k^2 + l^2)\hat{\psi}_1 \approx \hat{q}_1$  and  $-(k^2 + l^2)\hat{\psi}_2 \approx \hat{q}_2$ , i.e., the potential vorticity in each layer looks like the actual vorticity in that layer, and the layers are nearly decoupled. For disturbances whose horizontal scale is much larger than the Rossby length ( $k^2 + l^2 \ll 2\mu^2$ ), (19.47) and (19.48) reduce to  $-(k^2 + l^2)\hat{\psi}_1 \approx 1/2(\hat{q}_1 + \hat{q}_2)$  and  $-(k^2 + l^2)\hat{\psi}_2 \approx 1/2(\hat{q}_1 + \hat{q}_2)$ , i.e., the vorticity in each layer depends equally on the potential vorticity in both layers, and the layers are strongly coupled. Since baroclinic instability depends on the coupling of the counterpropagating Rossby waves in the two layers, we might expect baroclinic instability to be absent for short waves. This will indeed turn out to be the case. Continuing our analysis, we now substitute (19.47) and (19.48) into (19.43) and (19.44) to obtain

$$\begin{pmatrix} c - U + \bar{q}_{1y} \left[ \frac{k^2 + l^2 + \mu^2}{(k^2 + l^2)(k^2 + l^2 + 2\mu^2)} \right] & \bar{q}_{1y} \left[ \frac{\mu^2}{(k^2 + l^2)(k^2 + l^2 + 2\mu^2)} \right] \\ -\bar{q}_{1y} \left[ \frac{\mu^2}{(k^2 + l^2)(k^2 + l^2 + 2\mu^2)} \right] & c + U - \bar{q}_{1y} \left[ \frac{k^2 + l^2 + \mu^2}{(k^2 + l^2)(k^2 + l^2 + 2\mu^2)} \right] \end{pmatrix} \begin{pmatrix} \hat{q}_1 \\ \hat{q}_2 \end{pmatrix} = 0. \tag{19.49}$$

This pair of equations can be regarded as a concise mathematical description of the interaction of two counterpropagating Rossby waves. The upper right term in the matrix of (19.49) gives the effect of the lower potential vorticity anomaly on the behavior of the upper layer, while the lower left term in the matrix gives the effect of the upper potential vorticity anomaly on the behavior of the lower layer. Note that the effect of these interactions decays with increasing wavenumber and decreasing  $\bar{q}_{1y}$  according to  $\bar{q}_{1y}[\mu^2/(k^2 + l^2)(k^2 + l^2 + 2\mu^2)]$ . If the basic state poleward potential vorticity gradient in the lower layer were not present, the Rossby wave in the upper layer would propagate with phase speed  $c = U - \bar{q}_{1y}[(k^2 + l^2 + \mu^2)/(k^2 + l^2)(k^2 + l^2 + 2\mu^2)]$ . Similarly, if the basic state poleward potential vorticity gradient in the upper layer were not present, the Rossby wave in the lower layer would propagate with phase speed  $c = -U + \bar{q}_{1y}[(k^2 + l^2 + \mu^2)/(k^2 + l^2)(k^2 + l^2 + 2\mu^2)]$ .

Regarding (19.49) as a linear homogeneous system in the unknowns  $\hat{q}_1$  and  $\hat{q}_2$ , we require that the determinant of the coefficients vanish, which yields, for unstable waves, the condition  $k^2 + l^2 < 2\mu^2$ , in which case

$$c_i = \pm U \left[ \frac{2\mu^2 - k^2 - l^2}{2\mu^2 + k^2 + l^2} \right]^{1/2}. \tag{19.50}$$

The growth rate is  $kc_i$ , and the fastest growing wave occurs for  $l = 0$ . Taking  $d(kc_i)/dk = 0$ , we find that the fastest growing wave has

$$k = \pm \left( 2^{1/2} - 1 \right)^{1/2} (2\mu^2)^{1/2} \approx \pm \mu 0.6436 (2\mu^2)^{1/2}. \tag{19.51}$$

When (19.51) is substituted in (19.50) we find that the fastest growth rate is

$$(kc_i)_{\max} = (2 - 2^{1/2}) U \mu \approx 0.5859 U \mu. \quad (19.52)$$

---

### Problems

---

1. Derive the linearized potential vorticity equation (19.5) from the nonlinear potential vorticity equation (19.1).
2. Show that, under the assumptions of the Eady model, the basic state potential vorticity is uniform, and therefore that the disturbance potential vorticity vanishes.
3. From (19.26), prove that instability occurs when  $(N/f)H(k^2 + l^2)^{1/2} < 1.1997$ .
4. For the two-layer model, what does the eigenfunction corresponding to the eigenvalue (19.52) look like? Do the PV anomalies tilt against the basic state shear?